Chapter 4
Interfaces

We can define an interface between a reinforcement and a matrix as the bounding surface between the two, across which a discontinuity in some parameter occurs. The discontinuity across the interface may be sharp or gradual. Mathematically, interface is a bidimensional region. In practice, we have an interfacial region with a finite thickness. In any event, an interface is the region through which material parameters, such as concentration of an element, crystal structure, atomic registry, elastic modulus, density, coefficient of thermal expansion, etc., change from one side to another. Clearly, a given interface may involve one or more of these items.

The behavior of a composite material is a result of the combined behavior of the following three entities:

- Fiber or the reinforcing element
- Matrix
- Fiber/matrix interface

The reason the interface in a composite is of great importance is that the internal surface area occupied by the interface is quite extensive. It can easily go as high as 3,000 cm^2/cm^3 in a composite containing a reasonable fiber volume fraction. We can demonstrate this very easily for a cylindrical fiber in a matrix. The fiber surface area is essentially the same as the interfacial area. Ignoring the fiber ends, one can write the surface-to-volume ratio (S/V) of the fiber as

$$S/V = 2\pi rl/\pi r^2 l = 2/r, \tag{4.1}$$

where r and l are the fiber radius and length of the fiber, respectively. Thus, the surface area of a fiber or the interfacial area per unit volume increases as r decreases. Clearly, it is important that the fibers not be weakened by flaws because of an adverse interfacial reaction. Also, the applied load should be effectively transferred from the matrix to the fibers via the interface. Thus, it becomes extremely important to understand the nature of the interface region of any given composite system under a given set of conditions. Specifically, in the case

K.K. Chawla, *Composite Materials: Science and Engineering*,
DOI 10.1007/978-0-387-74365-3_4,

of a fiber reinforced composite material, the interface, or more precisely the interfacial zone, consists of near-surface layers of fiber and matrix and any layer (s) of material existing between these surfaces. Wettability of the fiber by the matrix and the type of bonding between the two components constitute the primary considerations. Additionally, one should determine the characteristics of the interface and how they are affected by temperature, diffusion, residual stresses, and so on. We discuss some of the interfacial characteristics and the associated problems in composites in a general way. The details regarding interfaces in polymer matrix, metal matrix, and ceramic matrix composites are given in specific chapters devoted to those composite types.

4.1 Wettability

Various mechanisms can assist or impede adhesion (Baier et al. 1968). A key concept in this regard is that of wettability. Wettability tells us about the ability of a liquid to spread on a solid surface. We can measure the wettability of a given solid by a liquid by considering the equilibrium of forces in a system consisting of a drop of liquid resting on a plane solid surface in the appropriate atmosphere. Figure 4.1 shows the situation schematically. The liquid drop will spread and wet the surface only if this results in a net reduction of free energy of the system. Note that a portion of the solid/vapor interface is substituted by the solid/liquid interface. Contact angle, θ, of a liquid on the solid surface fiber is a convenient and important parameter to characterize wettability. Commonly, the contact angle is measured by putting a sessile drop of the liquid on the flat surface of a solid substrate. The contact angle is obtained from the tangents along three interfaces: solid/liquid, liquid/vapor, and solid/vapor. The contact angle, θ can be measured directly by a goniometer or calculated by using simple trigonometric relationships involving drop dimensions. In theory, one can use the following expression, called Young's equation, obtained by resolving forces horizontally

$$\gamma_{SV} = \gamma_{LS} + \gamma_{LV} \cos\theta, \tag{4.2}$$

where γ is the specific surface energy, and the subscripts SV, LS, and LV represent solid/vapor, liquid/solid, and liquid/vapor interfaces, respectively. If this process of substitution of the solid/vapor interface involves an increase in the free energy of the system, then complete spontaneous wetting will not result. Under such conditions, the liquid will spread until a balance of forces acting on the surface is attained; that is, we shall have partial wetting. A small θ implies good wetting. The extreme cases are: $\theta = 0°$, corresponding to perfect wetting and $\theta = 180°$, corresponding to no wetting. In practice, it is rarely possible to obtain a unique equilibrium value of θ. Also, there exists a range of contact angles between the maximum or advancing angle, θ_a, and the minimum or receding angle, θ_r. This phenomenon, called the *contact-angle hysteresis*, is generally observed in

polymeric systems. Among the sources of this hysteresis are: chemical attack, dissolution, inhomogeneity of chemical composition of solid surface, surface roughness, and local adsorption.

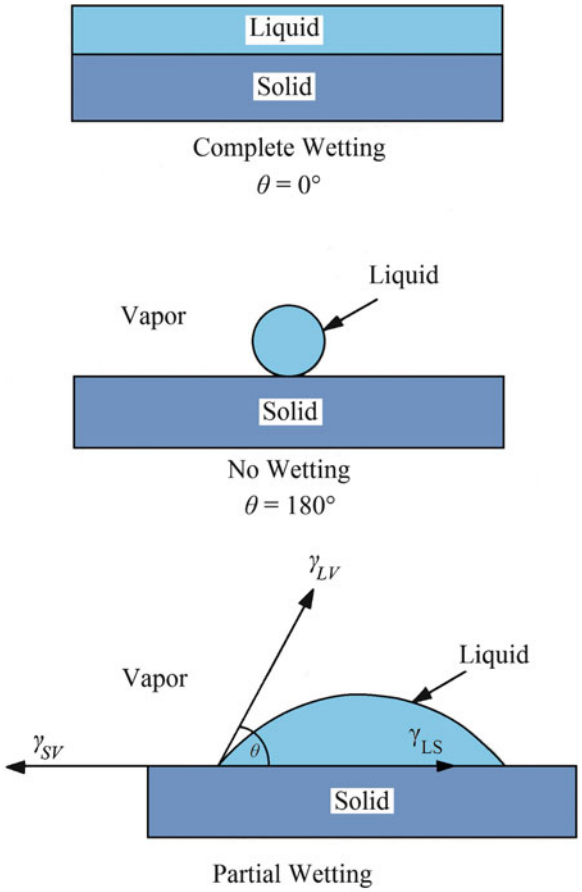

Fig. 4.1 Three different conditions of wetting: complete wetting, no wetting, and partial wetting

It is important to realize that wettability and bonding are not synonymous terms. Wettability describes the extent of intimate contact between a liquid and a solid; it does not necessarily mean a strong bond at the interface. One can have excellent wettability and a weak van der Waals-type low-energy bond. A low contact angle, meaning good wettability, is a necessary but not sufficient condition for strong bonding. Consider again a liquid droplet lying on a solid surface. In such a case, Young's equation, Eq. (4.1), is commonly used to express the equilibrium among surface tensions in the horizontal directions. What is normally neglected in such an analysis is that there is also a vertical force $\gamma_{\mathrm{LV}} \sin \theta$, which must be balanced by

a stress in the solid acting perpendicular to the interface. This was first pointed out by Bikerman and Zisman in their discussion of the proof of Young's equation by Johnson (1959). The effect of internal stress in the solid for this configuration was discussed by Cahn et al. (1964; 1979). In general, Young's equation has been applied to void formation in solids without regard to the precise state of internal stress. Fine et al. (1993) analyzed the conditions for occurrence of these internal stresses and their effect on determining work of adhesion in particle reinforced composites.

Wettability is very important in PMCs because in the PMC manufacturing the liquid matrix must penetrate and wet fiber tows. Among polymeric resins that are commonly used as matrix materials, thermoset resins have a viscosity in the 1–10 Pas range. The melt viscosities of thermoplastics are two to three orders of magnitude higher than those of thermosets and they show, comparatively, poorer fiber wetting characteristics. Although the contact angle is a measure of wettability, the reader should realize that its magnitude will depend on the following important variables: time and temperature of contact; interfacial reactions; stoichiometry, surface roughness and geometry; heat of formation; and electronic configuration.

Example 4.1 Consider a laminated composite made by laminating sheets of two materials (1 and 2), each of volume, v, in an alternating sequence. Let the thickness of the laminae of the two materials be t_1 and t_2, and the number of sheets of each be N_1 and N_2, respectively. For a given volume fraction of component 1, V_1 (remember that $V_1 + V_2 = 1$), derive an expression for the interfacial area as a function of t_1 and t_2.

Solution Let the area of cross section of the laminate be A. Let v, V, N, and t represent the volume, volume fraction, number, and thickness of the laminae, respectively, and let subscripts 1 and 2 denote the two components. Then, we can write

$$V_1 = \text{volume of component 1/total volume} = AN_1t_1/v$$
$$V_2 = \text{volume of component 2/total volume} = AN_2t_2/v$$
$$V_1 + V_2 = 1$$
$$A(N_1t_1/v + N_2t_2/v) = 1$$

or

$$A/v = 1/(N_1t_1 + N_2t_2) \tag{4.3}$$

$$\text{Total number of interfaces} = (N_1 + N_2 - 1)$$

$$\text{Total interfacial area per unit volume, } I_a = (N_1 + N_2 - 1)A/v. \tag{4.4}$$

From Eqs. (4.3) and (4.4), we have

$$I_a = (N_1 + N_2 - 1)/(N_1t_1 + N_2t_2).$$

Taking $t_1 = t_2 = t$, we get

$$I_a = (N_1 + N_2 - 1)/(N_1 + N_2)t = k/t,$$

where $k = (N_1 + N_2 - 1)/(N_1 + N_2) =$ a constant. The constant k will be approximately equal to 1 when N_1 and N_2 are very large compared to unity. Thus, the interfacial area is inversely proportional to the thickness of the laminae.

4.1.1 *Effect of Surface Roughness*

In the earlier discussion, it is implicitly assumed that the substrate is perfectly smooth. This, however, is far from true in practice. More often than not, the interface between fiber and matrix is rather rough instead of the ideal planar interface; see Fig. 4.2. Most fibers or reinforcements show some degree of roughness (Chawla 1998). Surface roughness profiles of the fiber surface obtained by atomic force microscopy (AFM) can provide detailed, quantitative information on the surface morphology and roughness of the fibers. It would appear that AFM can be a useful tool in characterizing the fiber surface roughness (Chawla et al. 1993, 1995; Jangehud et al. 1993; Chawla and Xu 1994). Figure 4.3 shows an example of roughness characterization by AFM of the surface of a polycrystalline alumina fiber (Nextel 610).

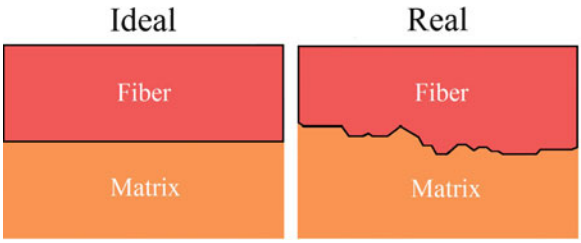

Fig. 4.2 (**a**) An ideal planar interface between reinforcement and matrix. (**b**) A more likely jagged interface between fiber and matrix

Generally, the fiber/matrix interface will assume the same roughness profile as that of the fiber. In the case of polymer matrix composites, an intimate contact at the molecular level between the fiber and the matrix brings inter-molecular forces into play with or without causing a chemical linkage between the components. In order to obtain an intimate contact between the fiber and the matrix, the matrix in liquid form must wet the fiber. Coupling agents are frequently used to improve the wettability between the components. At times, other approaches, such as modifying the matrix composition, are used. Wenzel (1936) discussed the effect of surface roughness on wettability and pointed out that "within a measured unit on a rough surface, there is actually more surface, and in a sense therefore a greater surface energy, than in the same measured unit area on a smooth surface." Following

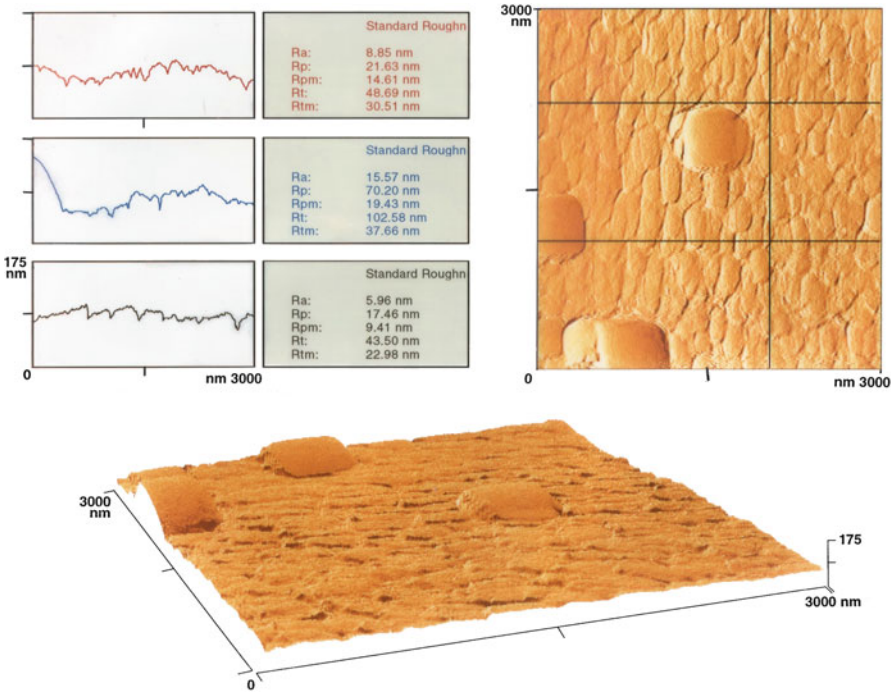

Fig. 4.3 Characterization of surface roughness of a polycrystalline alumina fiber (Nextel 610) by atomic force microscopy. The three profiles on the *left-hand side* correspond to the two horizontal and one vertical lines on the *right-hand side* figure. The *bottom figure* shows a three-dimensional perspective view of surface

Wenzel, the effect of surface roughness on wettability can be described in terms of r, the ratio of real area, A_{real}, to projected area, A_{proj}, of the interface. Thus,

$$\cos\ \theta_0 = r\frac{\gamma_{\text{SV}} - \gamma_{\text{LS}}}{\gamma_{\text{LV}}}, \tag{4.5}$$

where $r = A_{\text{real}}/A_{\text{proj}}$.

If $\theta_0 < 90^\circ$, wettability is enhanced by roughness, and if $\theta_0 > 90^\circ$, wettability is reduced by roughness. If wetting is poor ($\theta_0 > 90^\circ$), surface roughness can reduce bonded area and lead to void formation and possible stress concentrations.

4.2 Crystallographic Nature of Interface

Most of the physical, chemical, and mechanical discontinuities at the interface mentioned previously are self-explanatory. The concept of atomic registry or the crystallographic nature of an interface needs some elaboration. In terms of the types

of atomic registry, we can have a coherent, semicoherent, or incoherent interface. A *coherent* interface is one where atoms at the interface form part of both the crystal lattices; that is, there exists a one-to-one correspondence between lattice planes on the two sides of the interface. A coherent interface thus has some coherency strains associated with it because of the straining of the lattice planes in the two phases to provide the continuity at the interface to atomic sites on the two sides of the interface. In general, a perfect atomic registry does not occur between unconstrained crystals. Rather, coherency at the interface invariably involves an elastic deformation of the crystals. A coherent interface, however, has a lower energy than an incoherent one. A classic example of a coherent interface is the interface between Guinier–Preston (G-P) zones and the aluminum matrix. These G-P zones are precursors to the precipitates in aluminum matrix. With increasing size of the crystals, the elastic strain energy becomes more than the interfacial energy, leading to a lowering of the free energy of the system by introducing dislocations at the interface. Such an interface, containing dislocations to accommodate the large interfacial strains and thus having only a partial atomic registry, is called a *semicoherent interface*. Thus, a semicoherent interface is one that does not have a very large lattice mismatch between the phases, and the small mismatch is accommodated by the introduction of dislocations at the interface. As examples, we cite interfaces between a precipitate and a matrix as well as interfaces in some eutectic composites such as NiAl–Cr system (Walter et al. 1969), which has semicoherent interfaces between phases. With still further increases in crystal sizes, the dislocation density at the interface increases, and eventually the dislocations lose their distinct identity; that is, it is no longer possible to specify individual atomic positions at the interface. Such an interface is called an *incoherent interface*. An incoherent interface consists of such severe atomic disorder that no matching of lattice planes occurs across the boundary, i.e., no continuity of lattice planes is maintained across the interface. This eliminates coherency strains, but the energy associated with the boundary increases because of severe atomic disorder at the grain boundary. The atoms located at such an interface do not correspond to the structure of either of the two crystals or grains. Crystallographically, most of the interfaces that one encounters in fiber, whisker, or particle reinforced composites are incoherent.

4.3 Interactions at the Interface

We mentioned earlier that interfaces are bidimensional regions. An initially planar interface, however, can become an interfacial zone with, possibly, multiple interfaces resulting from the formation of different intermetallic compounds, interdiffusion, and so on. In such a case, in addition to the compositional parameter, we need other parameters to characterize the interfacial zone: for example, geometry and dimensions; microstructure and morphology; and mechanical, physical, chemical, and thermal characteristics of different phases present in the interfacial zone. It commonly occurs that initially the components of a composite system are chosen

on the basis of their mechanical and physical characteristics in isolation. It is important to remember, however, that when one puts together two components to make a composite, the composite will rarely be a system in thermodynamic equilibrium. More often than not, there will be a driving force for some kind of interfacial reaction(s) between the two components, leading to a state of thermodynamic equilibrium for the composite system. Of course, thermodynamic information, such as phase diagrams, can help predict the final equilibrium state of the composite. For example, data regarding reaction kinetics, diffusivities of one constituent in another, etc. can provide information about the rate at which the system would tend to attain the equilibrium state. In the absence of thermodynamic and kinetic data, experimental studies would have to be done to determine the compatibility of the components. Quite frequently, the very process of fabrication of a composite can involve interfacial interactions that can cause changes in the constituent properties and/or interface structure. For example, if the fabrication process involves cooling from high temperatures to ambient temperature, the difference in the expansion coefficients of the two components can give rise to thermal stresses of such a magnitude that the softer component (generally the matrix) will deform plastically. Chawla and Metzger (1972) showed in a tungsten fiber/single crystal copper matrix (nonreacting components) that liquid copper infiltration of tungsten fibers at about 1,100 °C followed by cooling to room temperature resulted in a dislocation density in the copper matrix that was much higher in the vicinity of the interface than away from the interface. The high dislocation density in the matrix near the interface occurred because of plastic deformation of the matrix caused by high thermal stresses near the interface. Arsenault and coworkers (Arsenault and Fisher 1983; Vogelsang et al. 1986) found similar results in SiC whisker/aluminum matrix composite. Many other researchers have observed dislocation generation in the vicinity of reinforcement/matrix interface due to the thermal mismatch between the reinforcement and metal matrix. In PMCs and CMCs, the matrix is unlikely to deform plastically in response to the thermal stresses. It is more likely to relieve those stresses by matrix microcracking. In powder processing techniques, the nature of the powder surface will influence the interfacial interactions. For example, an oxide film, which is invariably present on the surface of powder particles, will affect the chemical nature of the powder. Topographic characteristics of the components can also affect the degree of atomic contact that can be obtained between the components. This can result in geometrical irregularities (e.g., asperities and voids) at the interface, which can be a source of stress concentrations.

Example 4.2 Distinguish between the terms *surface energy* and *surface tension*.

Answer Surfaces in solids and liquids have special characteristics because surfaces represent the termination of the phase. Consider an atom or a molecule in the interior of an infinite solid. It will be bonded in all directions, and this balanced bonding results in a reduced potential energy of the system. At a free surface, atoms or molecules are not surrounded by other atoms or molecules on all sides; they have bonds or neighbors on only one side. Thus there exists an

imbalance of forces at the surface (it is true at any interface, really) that results in a rearrangement of atoms or molecules at the surface. We say that a surface has an extra energy called *surface energy*, i.e., surface energy is the excess energy per unit area associated with the surface because of the unsatisfied bonds at the surface. The units of surface energy are J m^2. We can also define it as the energy needed to create a unit surface area. Surface energy depends on the crystallographic orientation. For example, if we hold a single crystal at high temperature, it will assume a shape bounded by low-energy crystallographic planes of minimum surface energy. *Surface tension* is the tendency to minimize the total surface energy by minimizing the surface area. Surface energy and surface tension are numerically equal for isotropic materials. Surface tension is generally given in units of N/m, which is the same as J m^2. This is not true for anisotropic solids. Consider a surface of area A with a surface energy of γ. If we increase the surface area by a small amount, the work done per unit increase of area can be written as

$$\mathrm{d}(A\gamma)/\mathrm{d}A = \gamma + \partial\gamma/\partial A.$$

The term $\partial\gamma/\partial A$ is zero for liquids because of atomic or molecular mobility in the liquid state. The structure of a liquid surface is unchanged when we increase its surface area. Actually, for any material that is incapable of withstanding shear, $\partial\gamma/\partial A = 0$. In general, such materials include liquids and solids at high temperatures. Thus, for a liquid, the surface tension and surface energy are equal. Because, thermodynamically, the most stable state is the one with a minimum of free energy, isotropic liquids tend toward a minimum area/unit volume, i.e., a sphere. Such equality does not hold for solids that can withstand shear. If we stretch the surface of a solid, the atoms or molecules at the surface are pulled apart, γ decreases, and the quantity $\partial\gamma/\partial A$ becomes negative. Thus, for solids, the surface tension is not equal to surface energy. That is why a piece of solid metal does not assume a spherical shape when left to stand at room temperature. In fact, the surface energy of a crystal varies with crystallographic orientation. Generally, the more densely packed planes have a lower surface energy, and they end up forming the stable planes on the surface.

Typically, polymers have surface energies <100 mJ m^2; oxides have between 100 and 2,000 mJ m^2, while metals, carbides, nitrides have $>1{,}000$ mJ m^2.

4.4 Types of Bonding at the Interface

It is important to be able to control the degree of bonding between the matrix and the reinforcement. To do so, it is necessary to understand all the different possible bonding types, one or more of which may be acting at any given instant. We can conveniently classify the important types of interfacial bonding as follows:

- Mechanical bonding
- Physical bonding
- Chemical bonding

- Dissolution bonding
- Reaction bonding

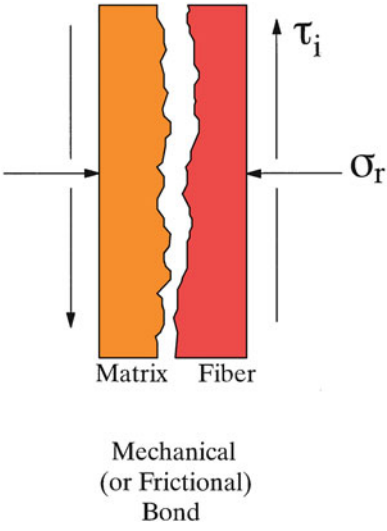

Fig. 4.4 Mechanical gripping due to radial shrinkage of a matrix in a composite being more than that of the fiber on cooling from a high temperature

4.4.1 Mechanical Bonding

Simple mechanical keying or interlocking effects between two surfaces can lead to a considerable degree of bonding. In a fiber reinforced composite, any contraction of the matrix onto a central fiber would result in a gripping of the fiber by the matrix. Imagine, for example, a situation in which the matrix in a composite radially shrinks more than the fiber on cooling from a high temperature. This would lead to a gripping of the fiber by the matrix even in the absence of any chemical bonding (Fig. 4.4). The matrix penetrating the crevices on the fiber surface, by liquid or viscous flow or high-temperature diffusion, can also lead to some mechanical bonding. In Fig. 4.4, we show a radial gripping stress, σ_r. This is related to the interfacial shear stress, τ_i, as

$$\tau_i = \mu\sigma_r, \tag{4.6}$$

where μ is the coefficient of friction, generally between 0.1 and 0.6.

In general, mechanical bonding is a low-energy bond vis à vis a chemical bond, i.e., the strength of a mechanical bond is lower than that of a chemical bond. Work on metallic wires in metal matrices (Vennett et al. 1970; Schoene and Scala 1970) indicates that in the presence of interfacial compressive forces, a metallurgical bond

is not quite necessary because the mechanical gripping of the fibers by the matrix is sufficient to cause an effective reinforcement, as indicated by the occurrence of multiple necking in fibers when the composite is pulled in tension. Hill et al. (1969) confirmed the mechanical bonding effects in tungsten filament/aluminum matrix composites. Chawla and Metzger (1978) studied bonding between an aluminum substrate and anodized alumina (Al_2O_3) films and found that with a rough interface a more efficient load transfer from the aluminum matrix to the alumina occurred. There is only mechanical bond between Al_2O_3 and Al. Pure mechanical bonding alone is not enough in most cases. However, mechanical bonding could add, in the presence of reaction bonding, to the overall bonding. Also, mechanical bonding is efficient in load transfer when the applied force is parallel to the interface. In the case of mechanical bonding, the matrix must fill the hills and valleys on the surface of the reinforcement. Rugosity, or surface roughness, can contribute to bond strength only if the liquid matrix can wet the reinforcement surface. A good example of excellent wetting (contact angle, $\theta = 0°$) is between WC and cobalt liquid. If, on the other hand, the matrix, liquid polymer or molten metal, is unable to penetrate the asperities on the fiber surface, then the matrix will solidify and leave interfacial voids, as shown in Fig. 4.5. Examples of surface roughness contributing to interfacial strength include:

1. Surface treatments of carbon fibers, e.g., nitric acid oxidation of carbon fibers, which increase specific surface area and lead to good wetting in PMCs, consequently an improved interlaminar shear strength (ILSS) of the composite (see Chap. 8).
2. Most metal matrix composites will have some roughness-induced mechanical bonding between the ceramic reinforcement and the metal matrix (see Chap. 6).
3. Most CMC systems also show a mechanical gripping between the fiber and the matrix (see Chap. 7).

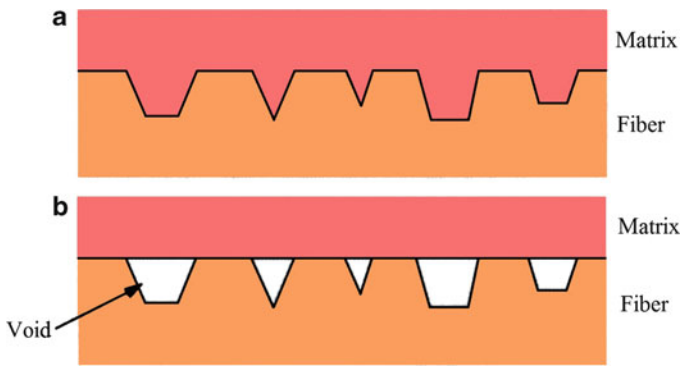

Fig. 4.5 (**a**) Good mechanical bond. (**b**) Lack of wettability can make a liquid polymer or metal unable to penetrate the asperities on the fiber surface, leading to interfacial voids

We can make some qualitative remarks about general interfacial characteristics that are desirable in different composites. In PMCs and MMCs, one would like to have mechanical bonding in addition to chemical bonding. In CMCs, on the other hand, it would be desirable to have mechanical bonding in lieu of chemical bonding. In any ceramic matrix composite, roughness-induced gripping at the interface is quite important. Specifically, in fiber reinforced ceramic matrix composites, interfacial roughness-induced radial stress will affect the interface debonding, the sliding friction between the fiber and the matrix during pullout of debonded fibers, and the fiber pullout length.

4.4.2 Physical Bonding

Any bonding involving weak, secondary or van der Waals forces, dipolar interactions, and hydrogen bonding can be classified as *physical bonding*. The bond energy in such physical bonding is very low, approximately 8–16 kJ/mol.

4.4.3 Chemical Bonding

Atomic or molecular transport, by diffusional processes, is involved in chemical bonding. Solid solution and compound formation may occur at the interface, resulting in a reinforcement/matrix interfacial reaction zone having a certain thickness. This encompasses all types of covalent, ionic, and metallic bonding. Chemical bonding involves primary forces and the bond energy is in the range of approximately 40–400 kJ/mol.

There are two main types chemical bonding:

1. *Dissolution bonding*. In this case, interaction between components occurs at an electronic scale. Because these interactions are of rather short range, it is important that the components come into intimate contact on an atomic scale. This implies that surfaces should be appropriately treated to remove any impurities. Any contamination of fiber surfaces, or entrapped air or gas bubbles at the interface, will hinder the required intimate contact between the components.
2. *Reaction bonding*. In this case, a transport of molecules, atoms, or ions occurs from one or both of the components to the reaction site, that is, the interface. This atomic transport is controlled by diffusional processes. Such a bonding can exist at a variety of interfaces, e.g., glass/polymer, metal/metal, metal/ceramic, or ceramic/ceramic.

Two polymer surfaces may form a bond owing to the diffusion of matrix molecules to the molecular network of the fiber, thus forming tangled molecular bonds at the interface. Coupling agents (silanes are the most common ones) are used for glass fibers in resin matrices; see Chap. 5 for details. Surface treatments

(oxidative or nonoxidative) are given to carbon fibers to be used in polymeric materials; we describe these in Chap. 5. In metallic systems, solid solution and intermetallic compound formation can occur at the interface. A schematic of the diffusion phenomenon between a fiber and a matrix resulting in solid solution as well as a layer of an intermetallic compound, M_xF_y is shown in Fig. 4.6. The plateau region of the interfacial zone, which has a constant proportion of the two atomic species, is the region of intermetallic compound formation. The reaction products and the reaction rates can vary, depending on the matrix composition, reaction time, and temperature. Generally, one tries to fit such data to an expression of the form

$$x^2 \approx Dt, \tag{4.7}$$

where x is the thickness of the reaction zone, D is the diffusivity, and t is the time. This expression follows from the theory of diffusion in solids. The diffusivity, D, depends on the temperature in an exponential manner

$$D = A \exp(-\Delta Q/kT), \tag{4.8}$$

where A is a preexponential constant, ΔQ is the activation energy for the rate-controlling process, k is Boltzmann's constant, and T is the temperature in kelvin. This relationship follows from the diffusion-controlled growth in an infinite diffusion couple with planar interface. For a composite containing cylindrical fibers of a small diameter, the diffusion distance is very small, i.e., the condition of an infinite diffusion couple with planar interface is not likely to be valid. However, to a first approximation, we can write

$$x^2 \approx ct, \tag{4.9}$$

where c is a pseudodiffusivity and has the dimensions of diffusivity (m^2/s). The reader should bear in mind that this approximate relationship can be expected to work for composites in which the reaction thickness is small compared to the interfiber spacing. Under these conditions, one can use an Arrhenius-type relationship, $c = B \exp(-\Delta Q/kT)$, where B is a preexponential constant. A plot of ln c vs. $1/T$ can be used to obtain the activation energy, ΔQ, for a fiber/matrix reaction in a given temperature range. The preexponential constant, the constant B, depends on the matrix composition, fiber, and the environment.

4.5 Optimum Interfacial Bond Strength

Two general ways of obtaining an optimum interfacial bond involve treatments of fiber or reinforcement surface or modification of matrix composition. It should be emphasized that maximizing the bond strength is not always the goal. In brittle

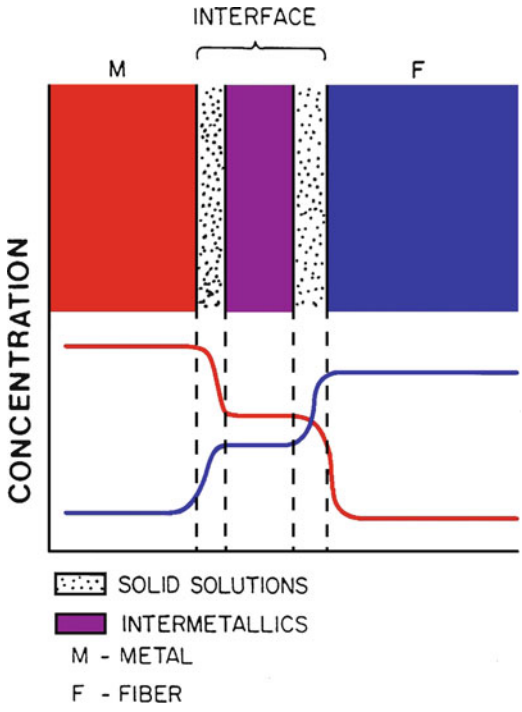

Fig. 4.6 Interface zone in a metal matrix composite showing solid solution and intermetallic compound formation

matrix composites, too strong a bond would cause embrittlement. We can illustrate the situation by examining the following three cases.

4.5.1 Very Weak Interface or Fiber Bundle (No Matrix)

This extreme situation will prevail when we have no matrix and the composite consists of only a fiber bundle. The bond strength in such a composite will only be due to interfiber friction. A statistical treatment of fiber bundle strength (see Chap. 12) shows that the fiber bundle strength is about 70–80 % of average single-fiber strength.

4.5.2 Very Strong Interface

The other extreme in interfacial strength is when the interface is as strong or stronger than the higher-strength component of the composite, generally the reinforcement. In this case, of the three components—reinforcement, matrix, and interface—the interface will have the lowest strain-to-failure. The composite will fail when any cracking occurs at a weak spot along the brittle interface. Typically, in such a case, a catastrophic failure will occur, and we will have a composite with very low toughness.

4.5.3 Optimum Interfacial Bond Strength

An interface with an optimum interfacial bond strength will result in a composite with an enhanced toughness, but without a severe penalty on the strength parameters. Such a composite will have multiple failure sites, most likely spread over the interfacial area, which will result in a diffused or global spread of damage, rather than a very local damage.

4.6 Tests for Measuring Interfacial Strength

Numerous tests have been devised to characterize the fiber/matrix interface strength. We briefly describe some of these.

4.6.1 Flexural Tests

Flexural or bend tests are very easy to do and can be used to get a semiqualitative idea of the fiber/matrix interfacial strength of a composite. There are two basic governing equations for a simple beam elastically stressed in bending:

$$\frac{M}{I} = \frac{E}{R} \tag{4.10}$$

and

$$\frac{M}{I} = \frac{\sigma}{y}, \tag{4.11}$$

where M is the applied bending moment, I is the second moment of area of the beam section about the neutral plane, E is the Young's modulus of elasticity of the material, R is the radius of curvature of the bent beam, and σ is the tensile or compressive stress on a plane distance y from the neutral plane. For a uniform, circular section beam

$$I = \frac{\pi d^4}{64}, \tag{4.12}$$

where d is the diameter of the circular section beam. For a beam of a uniform, rectangular section, we have

$$I = \frac{bh^3}{12}, \tag{4.13}$$

where b is the beam width and h is the height of the beam. Bending takes place in the direction of the depth, i.e., h and y are measured in the same direction. Also, for a beam with symmetrical section with respect to the neutral plane, replacing y in Eq. (4.11) by $h/2$ gives the stress at the beam surface. When an elastic beam is bent, the stress and strain vary linearly with thickness, y across the section, with the neutral plane representing the zero level. The material on the outside or above the neutral plane of the bent beam is stressed in tension while that on the inside or below the neutral plane is stressed in compression. In the elastic regime, the stress and strain are related by

$$\sigma = E\varepsilon. \tag{4.14}$$

From Eqs. (4.10), (4.11), and (4.14) we can obtain the following simple relation valid in the elastic regime:

$$\varepsilon = \frac{y}{R}. \tag{4.15}$$

Thus, the strain ε in a beam bent to a radius of curvature R varies linearly with distance y from the neutral plane across the beam thickness. We describe some variants of flexural tests.

4.6.1.1 Three-Point Bending

The bending moment in three-point bending is given by

$$M = \frac{P}{2} \times \frac{S}{2} = \frac{PS}{4}, \tag{4.16}$$

where P is the load and S is the span. The important point to note is that the bending moment in a three-point bend test increases from the two extremities of the beam to a maximum value at the midpoint, i.e., the maximum stress is reached along a line at the center of the beam. From Eqs. (4.11), (4.13), and (4.16), and taking $y = h/2$, we get the following expression for the maximum stress for a rectangular beam in three-point bending:

$$\sigma = \frac{6PS}{4bh^2} = \frac{3PS}{2bh^2}, \tag{4.17}$$

where b and h are breadth and height of the beam, respectively. We can have the fibers running parallel or perpendicular to the specimen length. When the fibers are running perpendicular to the specimen length, we obtain a measure of transverse strength of the fiber/matrix interface.

The shear stress in a three-point bend test is constant. The maximum in shear stress, τ_{max} will correspond to the maximum in load P_{max} and is given by

$$\tau_{max} = \frac{3P_{max}}{4bh}. \tag{4.18}$$

4.6.1.2 Four-Point Bending

This is also called *pure bending* because there are no transverse shear stresses on the cross sections of the beam between the two inner loading points. For an elastic beam bent in four-point, the bending moment increases from zero at the two extremities to a constant value over the inner span length. This bending moment in four-point is given by

$$M = \frac{P}{2} \times \frac{S}{4} = \frac{PS}{8} \tag{4.19}$$

where S is the outer span and the stress can be written as

$$\sigma = \frac{6PS}{8bh^2} = \frac{3PS}{4bh^2}. \tag{4.20}$$

4.6.1.3 Short-Beam Shear Test (Interlaminar Shear Stress Test)

This test is a special longitudinal three-point bend test with fibers parallel to the length of the bend bar and the length of the bar being very small. It is also known as the *i*nter*l*aminar *s*hear *s*trength (ILSS) test. The maximum shear stress, τ, occurs at the midplane and is given by Eq. (4.18). The maximum tensile stress occurs at the outermost surface and is given by Eq. (4.17). Dividing Eq. (4.18) by (4.17), we get

$$\frac{\tau}{\sigma} = \frac{h}{2S}. \tag{4.21}$$

Equation (4.21) says that if we *make the load span, S, very small*, we can maximize the shear stress, τ, so that the specimen fails under shear with a crack running along the midplane. Hence, we sometimes call this test as the short beam shear test.

The reader should bear in mind that the interpretation of this test is not straightforward. Clearly, the test becomes invalid if the fibers fail in tension before shear-induced failure occurs. The test will also be invalid if shear and tensile

failure occur simultaneously. It is advisable to make an examination of the fracture surface after the test to ensure that the crack is along the interface and not through the matrix. This test is standardized by ASTM (D2344). Among the advantages of this test are the following:

- Simple test, short span ($S = 5h$).
- Easy specimen preparation.
- Good for qualitative assessment of interfacial coatings.

The main disadvantages of this test are the following:

- Meaningful quantitative results on the fiber/matrix interface strength are difficult to obtain.
- It is difficult to ensure a pure shear failure along the interface.

4.6.1.4 Iosipescu Shear Test

This is a special test devised for measuring interfacial shear strength (Iosipescu 1967). In this test, a double-edged notched specimen is subjected to two opposing force couples. This is a special type of four-point bend test in which the rollers are offset, as shown in Fig. 4.7, to accentuate the shear deformation. A state of almost pure and constant shear stress is obtained across the section between the notches by selecting a proper notch angle (90°) and notch depth (22 % of full width). The average shear stress in this configuration is given by

$$\tau = \frac{P}{bh}, \tag{4.22}$$

where the symbols have the usual significance. The main advantage of this test is that a large region of uniform shear is obtained vis à vis other tests. However, there can be a substantial stress concentration near the notch tip in orthotropic materials (not so in isotropic materials) such as fiber reinforced composites. The stress concentration is proportional to the fiber orientation and the fiber volume fraction.

4.6.2 Single Fiber Pullout Tests

Single fiber pullout and pushout tests have been devised to measure interfacial characteristics. They frequently result in a peak load corresponding to fiber/matrix debonding and a frictional load corresponding to the fiber pullout from the matrix. The mechanics and interpretation of these tests are rather involved, and knowledge of the underlying assumptions is important in order to get useful information from such tests. We describe the salient features of these tests.

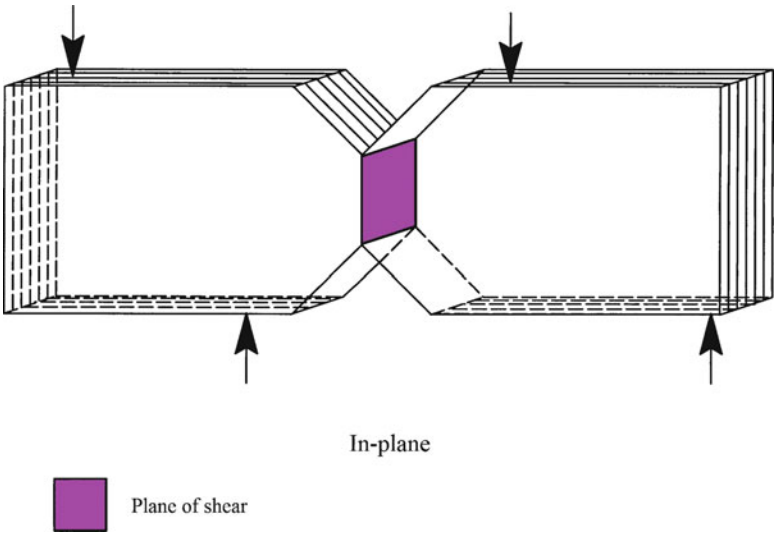

Fig. 4.7 A special type of four-point bend test, called the Iosipescu test, in which the rollers (position indicated by *arrows*) are offset to accentuate the shear deformation

These tests can provide useful information about the interface strength in model composite systems. They are not very helpful in the case of commercially available composites. One must also carefully avoid any fiber misalignment and introduction of bending moments. The mechanics of the single fiber pullout test are rather complicated (Chamis 1974; Penn and Lee 1989; Kerans et al. 1989; Marshall et al. 1992; Kerans and Parthasarathy 1991).

The fabrication of the single fiber pullout test sample is often the most difficult part; it entails embedding a part of the single fiber in the matrix. A modified variation of this simple method is to embed both ends of the single fiber in the matrix material, leaving the center region of the fiber uncovered. In all of these methods, the fiber is pulled out of the matrix in a tensile testing machine and a load vs. displacement record is obtained.

The peak load corresponds to the initial debonding of the interface. This is followed by frictional sliding at the interface, and finally by the fiber pullout from the matrix, during which a steady decrease in the load with displacement is observed. The steady decrease in the load is attributed to the decreasing area of the interface as the fiber is pulled out. Thus, the test simulates the fiber pullout that may occur in the actual composite, and more importantly, provides the bond strength and frictional stress values.

The effect of different Poisson's contractions of fiber and matrix can result in a radial tensile stress at the interface (see Chap. 10). The radial tensile stress will no doubt aid the fiber/matrix debonding process. The effect of Poisson's contraction, together with the fact that the imposed shear stress is not constant along the interface, complicates the analysis of the fiber pullout test.

These tests, however, can provide useful quantitative information about the interface strength in model composite systems. One must also carefully avoid any fiber misalignment and introduction of bending moments. Figure 4.8a shows the experimental setup for such a test. A portion of fiber, length l, is embedded in a matrix and a pulling tensile force is applied as shown. If we measure the stress required to pull the fiber out of the matrix as a function of the embedded fiber length, we get the plot shown in Fig. 4.8b. The stress required to pull the fiber out, without breaking it, increases linearly with the embedded fiber length, up to a critical length, l_c. At embedded fiber lengths greater than or equal to l_c, the fiber will fracture under the action of the tensile stress, σ, acting on the fiber. Consider Fig. 4.8a again. The tensile stress, σ, acting on the fiber results in a shear stress, τ, at the fiber/matrix interface. A simple force balance along the fiber length gives

$$\sigma\pi r^2 = \tau 2\pi r l.$$

For $l < l_c$, the fiber is pulled out and the interfacial shear strength is given by

$$\tau = \frac{\sigma r}{2l}. \tag{4.23}$$

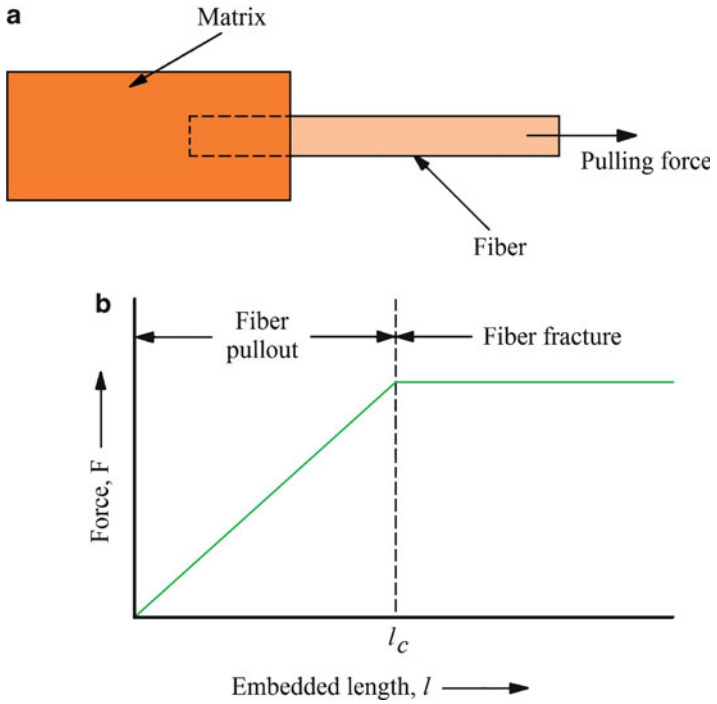

Fig. 4.8 (**a**) An experimental setup for a single fiber pullout test. A portion of fiber, length l, is embedded in a matrix and a pulling tensile force is applied as shown. (**b**) The stress required to pull the fiber out of the matrix as a function of the embedded fiber length

At $l > l_c$, fiber failure rather than pullout occurs. One measures the load required to debond as a function of the embedded fiber length. Then we can write

$$P = 2\pi r l \tau \tag{4.24}$$

and the interfacial shear strength, τ, can be calculated from the slope of the P vs. l. There is an implicit assumption in this analysis, viz., the shear stress acting along the fiber/matrix interface is a constant. In a single fiber embedded test, one obtains the average the load value over the entire interfacial surface area to get the interfacial debond strength and/or frictional strength. Analytical and finite element analyses show that the shear stress is a maximum close to the surface ends and falls rapidly within a distance of a few fiber diameters. Thus, one would expect the interface debonding to start near the surface and progressively propagate along the embedded length.

The interfacial shear strength is a function of the coefficient of friction, μ, and any normal compressive stress at the interface, σ_r. The source of radial compressive stress is the shrinkage of the matrix during cooling from the processing temperature.

4.6.3 Curved Neck Specimen Test

This technique was devised for PMCs. A special mold is used to prepare a curved neck specimen of the composite containing a single fiber along its central axis. The specimen is compressed and the fiber/matrix debonding is observed visually. The curved neck shape of the specimen enhances the transverse tensile stress at the fiber/matrix interface. The transverse tensile stress leading to interface debonding results from the fact that the matrix and the fiber have different Poisson's ratios. If the matrix Poisson ratio, ν_m, is greater than that of the fiber, ν_f, then on compression, there will result a transverse tensile stress at the center of the neck and perpendicular to the interface whose *magnitude* is given by (Broutman 1969):

$$\sigma_i = \frac{\sigma(\nu_m - \nu_f)E_f}{\left[(1+\nu_m)E_f + \left(1 - \nu_f - 2\nu_f^2\right)E_m\right]}, \tag{4.25}$$

where σ is the net section compressive stress (i.e., load/minimum area), E is the Young's modulus, ν is the Poisson's ratio, and the subscripts f and m denote fiber and matrix, respectively. Note the expression in (4.29) gives the magnitude of tensile stress developed perpendicular to the interface when the sample is subjected to a compressive load.

One can measure the net section stress, σ, corresponding to interface debonding and compute the interfacial tensile strength from (4.25). There are some important points that should be taken into account before using this test. One needs a special mold to prepare the specimen, and a very precise alignment of the fiber along the central axis is a must. Finally, a visual examination is required to determine the interface debonding point. This would limit the technique to transparent matrix materials. Acoustic emission detection techniques may be used to avoid visual examination.

4.6.4 *Instrumented Indentation Tests*

Many instrumented indentation tests have been developed that allow extremely small forces and displacements to be measured. Indentation instruments have been in use for hardness measurement for quite a long time, but depth sensing instruments with high resolution became available in the 1980s (Doerner and Nix 1986; Ferber et al. 1993, 1995; Janczak et al. 1997). Such instruments allow very small volumes of a material to be studied, and a very local characterization of microstructural variations is possible by mechanical means. Such an instrument records the total penetration of an indenter into the sample. The indenter position is determined by a capacitance displacement gage. Pointed or conical or rounded indenters can be used to displace a fiber aligned perpendicular to the composite surface. Figure 4.9 shows three different types of indenters available commercially: cylindrical with a flat end, conical with a flat end, and pointed. An example of fiber pushin is shown in a series of four photographs in Fig. 4.10. By measuring the applied force and displacement, interfacial stress can be obtained. The indenter can be moved toward the sample or away from the sample by means of a magnetic coil assembly. Such instruments are available commercially. One special instrument (Touchstone Res. Lab., Tridelphia, WV) combines an indentation system within the chamber of an SEM. Such an instrument combines the materials characterization ability of an SEM with a fiber pushout apparatus. Commonly, some assumptions are made in making an

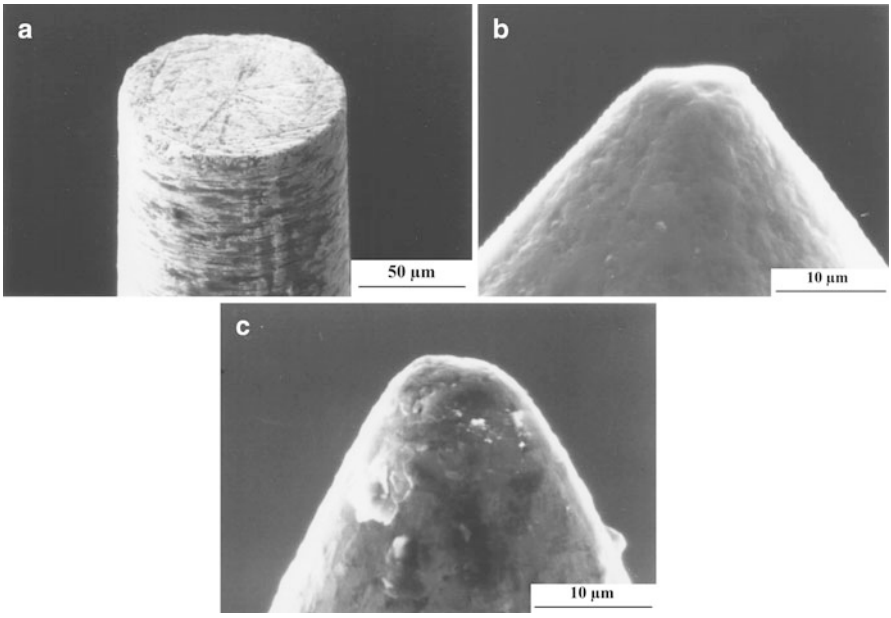

Fig. 4.9 Three different types of indenters: (**a**) cylindrical with a flat end, (**b**) conical with a flat end, and (**c**) pointed (courtesy of J. Janczak-Rusch and L. Rohr)

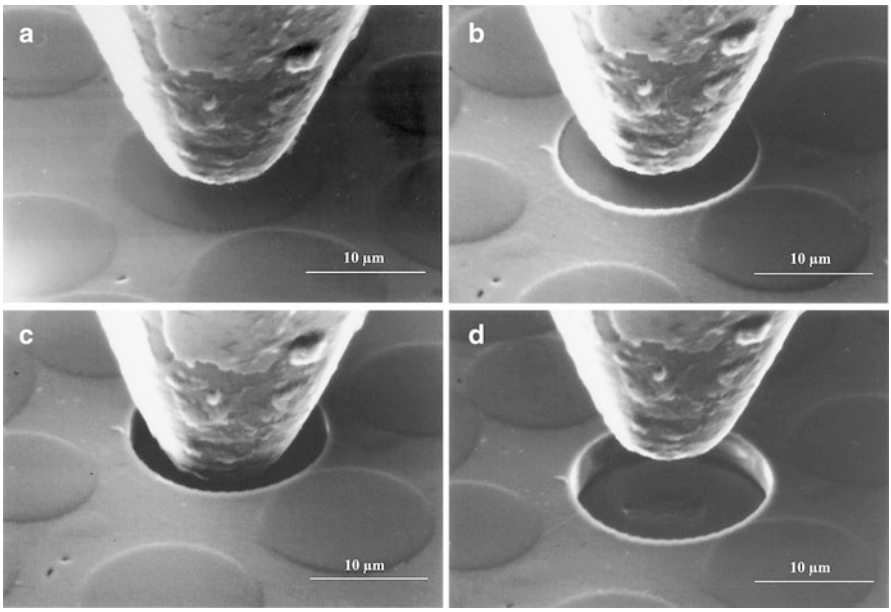

Fig. 4.10 An example of fiber pushin is shown in a series of four photographs. (**a**) Indenter approaching the fiber (**b**) touching the fiber (**c**) fiber pushin (**d**) lifting of indent (courtesy of J. Janczak-Rusch and L. Rohr)

interpretation of an indentation test to determine the strength characteristics of the interface region. For example:

1. Any elastic depression of the matrix adjacent to the fiber is negligible.
2. There are no surface stress concentrations.
3. There is no change in the fiber diameter due to the Poisson expansion during compression of the fiber.
4. There are no residual stresses.

The specimen thickness must be large compared to the fiber diameter for these assumptions to be valid.

Many methods involving the pressing of an indenter on a fiber cross section have been devised for measuring the interfacial bond strength in a fiber reinforced composite. The pushout test uses a thin specimen (1–3 mm), with the fibers aligned perpendicular to the viewing surface. The indenter is used to push a series of fibers out. Such a fiber pushout test can give the frictional shear stress, τ, acting at the fiber/matrix interface. An example of a valid pushout test, showing a three-region curve, is shown in Fig. 4.11. In the first region, the indenter is in the contact with the fiber and the fiber sliding is less than the specimen thickness t. This is followed by a horizontal region in which fiber sliding length is greater than or equal to

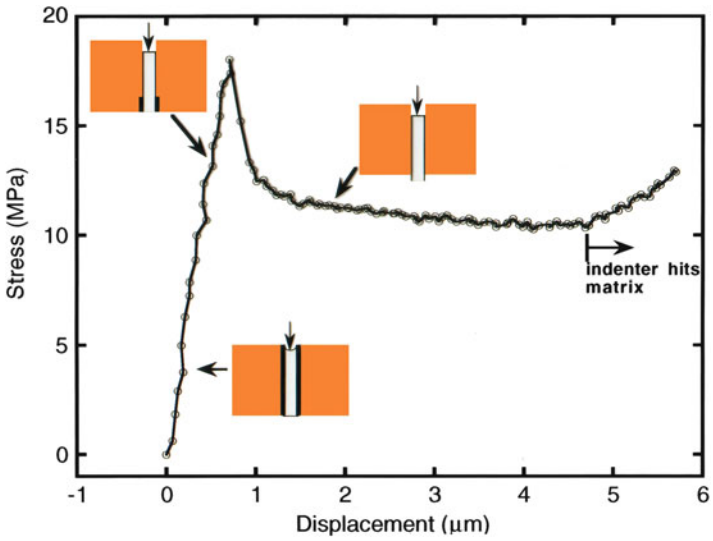

Fig. 4.11 Stress vs. displacement obtained in fiber pushout test (Chawla et al. 2001)

the sample thickness. In the third region, the indenter comes in contact with the matrix. In the horizontal region, the interfacial shear stress is given by:

$$\tau_i = \frac{P}{2\pi r t},$$

where P is the applied load, r is the fiber radius, and t is the specimen thickness. The specimen thickness should be much greater that the fiber diameter for this relationship to be valid. In the third region of Fig. 4.11 the value of the interfacial shear stress cannot be determined because the indenter comes in contact with the matrix, i.e., the test is no more valid.

In such indentation tests, after interfacial debonding, the fiber will slide along the interface over a distance that is dependent on the load applied by the indenter. The fiber is elastically compressed by the indenter load over the debonded length, which is assumed to be dependent on the interfacial friction. The axial load on the indenter is assumed to be balanced by the frictional stress at the interface, and the effect of radial expansion during indentation is neglected. There are two analytical models due to Kerans and Parthasarathy (1991) and Hsueh (1992) that take into account progressive debonding and sliding during fiber pushin and pushout. Radial and axial stresses are taken into account in both models and Coulombic friction is assumed at the fiber/matrix interface. Lara-Curzio and Ferber (1994) found that the two models gave almost identical results in Nicalon fiber/calcium aluminosilicate matrix composites.

An instrumented indentation test to be used at high temperature was developed by Eldridge (1995). Such a test is very useful for CMCs. Such a test is also useful to analyze the effect of residual stresses.

4.6.5 *Fragmentation Test*

In this test, a single fiber is embedded in a dog-bone-type tensile sample of matrix. When a tensile load is applied to such a sample, the load is transferred to the fiber via shear strains and stresses produced on planes parallel to the fiber/matrix interface. We discuss the subject of load transfer in fiber reinforced composites in Chap. 10. When the tensile stress in the fiber reaches its ultimate strength, it fragments into two parts. If we continue loading, this process of fiber fragmentation continues, i.e., the single fiber continues to fragment into even smaller pieces until the fiber fragment length becomes too small to enable loading it to fracture. This fiber length is called the *critical length,* l_c. This is shown schematically in Fig. 4.12. From a consideration of equilibrium of forces over an element dx of the fiber (see Chap. 10 also), we can write

$$\begin{aligned} \pi r^2 \, \mathrm{d}\sigma &= 2\pi r \, \mathrm{d}x\tau \\ \mathrm{d}\sigma/\mathrm{d}x &= 2\tau/r. \end{aligned} \tag{4.26}$$

where σ is the tensile stress, τ is the shear stress, and π is the fiber radius.

From Eq. (4.26), we obtain the critical length as follows. For simplicity, we consider that the matrix is perfectly plastic, i.e., we ignore any strain hardening effects and that the matrix yields in shear at shear stress of τ_y. We also assume that the shear stress along the fiber/matrix interface is constant over the length of the fiber fragment, l_c. Integrating Eq. (4.30), we get

$$\begin{aligned} \int_0^{\sigma_{\max}} \mathrm{d}\sigma &= \int_0^{l_c/2} 2\tau \, \mathrm{d}x/r \\ \sigma^{\max} &= \tau l_c/r \end{aligned} \tag{4.27}$$

or

$$\tau = \sigma^{\max} r/l_c = \sigma^{\max} d/2l_c. \tag{4.28}$$

The fiber fragmentation technique is a simple technique that gives us a quantitative measure of the fiber/matrix interfacial strength. Drzal et al. (1983, 1994, 1997) and others have used this technique extensively to characterize carbon fiber reinforced polymer matrix composites. Clearly, a transparent matrix is required. The technique will work only if the fiber failure strain is less than that of the matrix,

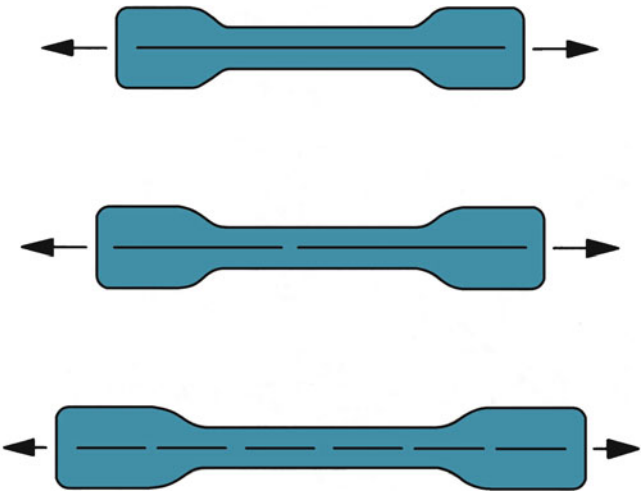

Fig. 4.12 A single-fiber fragmentation test. On loading the composite, the load is transferred to the fiber and on continued loading it fragments into smaller pieces until the fiber fragment length becomes too small to enable loading it to fracture

which is commonly true. The major shortcoming or the doubtful assumption is that the interfacial shear stress is constant over the fiber length. In addition, the real material is rarely perfectly plastic.

4.6.6 Laser Spallation Technique

Gupta et al. (1990, 1992) devised a laser spallation technique to determine the tensile strength of a planar interface between a coating (thickness > 0.5 μm) and a substrate. Figure 4.13 shows their experimental setup. A collimated laser pulse impinges on a thin film sandwiched between the substrate and a confining plate. This plate is made of fused quartz, which is transparent to Nd:YAG laser (wavelength $= 1.06$ μm). An aluminum film is used as the laser-absorbing medium. Absorption of the laser energy in the constrained aluminum film causes a sudden expansion of the film, which produces a compressive shock wave in the substrate that moves toward the coating/substrate interface. When the compression pulse hits the interface, part of it is transmitted into the coating. This compressive pulse is reflected into a tensile pulse at the free surface of the coating. If this tensile pulse is of a sufficient magnitude, it will remove the coating from the substrate. A laser Doppler displacement interferometer is used to record the time rate of change displacement of the coating free surface as the compressive pulse is reflected. By means of a sophisticated digitizer equipment, it is possible to obtain

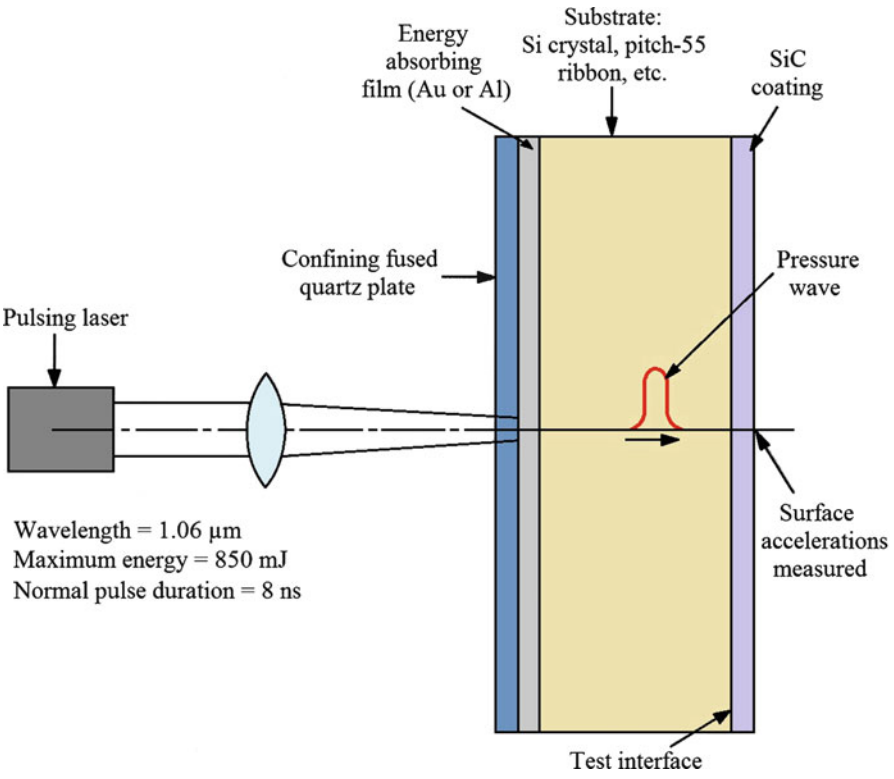

Fig. 4.13 Experimental setup for a laser spallation test. A collimated laser pulse impinges on a thin film sandwiched between the substrate and a confining plate. Absorption of the laser energy in the constrained aluminum film causes a sudden expansion of the film, which produces a compressive shock wave in the substrate that moves toward the coating/substrate interface. This compressive pulse is reflected into a tensile pulse at the free surface of the coating

a time resolution of about 0.5 ns for recording displacement fringes. This information is then related to the stress pulse history at the interface. A direct recording of the stress pulse makes this technique useful for interface systems involving ductile components. It is a complex technique and gives the strength of a flat interface.

References

Arsenault RJ, Fisher RM (1983) Scripta Met 17:67
Baier RE, Sharfin EG, Zisman WA (1968) Science 162:1360
Broutman LJ (1969). In: *Interfaces in Composites*, ASTM STP No. 452, American Society of Testing & Materials, Philadelphia, PA.
Cahn JW, Hanneman RE (1964) Surf Sci 94:65

Cahn JW (1979) In: Interfacial segregation. ASM, Metals Park, OH, p 3
Chamis CC (1974) In: Composite materials, vol 6. Academic, New York, p 32
Chawla KK (1997) Compos Interf 4:287
Chawla KK, Metzger M (1972) J Mater Sci 7:34
Chawla KK, Metzger M (1978) In: Advances in research on strength and fracture of materials, vol 3. Pergamon, New York, p 1039
Chawla KK, Xu ZR (1994) In: High performance composites: commonalty of phenomena. TMS, Warrendale, PA, p 207
Chawla KK, Xu ZR, Ha J-S, Lara-Curzio E, Ferber MK, Russ S (1995) Advances in ceramic matrix composites II. American Ceramic Society, Westerville, OH, p 779
Chawla KK, Xu ZR, Hlinak A, Chung Y-W (1993) In: Advances in ceramic-matrix composites. American Ceramic Society, Westerville, OH, p 725
Chawla N, Chawla KK, Koopman M, Patel B, Coffin C, Eldridge J (2001) Compos Sci Tech 61:1923
Doerner MF, Nix WD (1986) J Mater Res 1:601
Drzal LT, Madhukar M, Waterbury M (1994) Compos Sci Tech 27:65–71
Drzal LT, Rich MJ, Lloyd PF (1983) J Adhesion 16:1–30
Drzal LT, Sugiura N, Hook D (1997) Compos Interf 4:337
Eldridge JI (1995). Mat. Res. Soc. Symp. Proc., vol 365, Materials Research Society, p 283
Ferber MK, Wereszczak AA, Riester L, Lowden RA, Chawla KK (1993) In: Ceramic Sci. & Eng. Proc., Amer. Ceram. Soc., Westerville, OH
Ferber MK, Lara-Curzio E, Russ S, Chawla KK (1995) In: Ceramic matrix composites—advanced high-temperature structural materials. Materials Research Society, Pittsburgh, PA, p 277
Fine ME, Mitra R, Chawla KK (1993) Scripta Met Mater 29:221
Gupta V, Argon AS, Cornie JA, Parks DM (1990) Mater Sci Eng A126:105
Gupta V, Argon AS, Cornie JA, Parks DM (1992) J Mech Phys Solids 4:141
Hill RG, Nelson RP, Hellerich CL (1969) In: Proceedings of the refractory working group meeting, Seattle, WA, Oct
Hsueh C-H (1992) J Am Ceram Soc 76:3041
Iosipescu N (1967) J Mater 2:537
Janczak J, Bürki G, Rohr L (1997) Key Eng Mater 127:623
Jangehud I, Serrano AM, Eby RK, Meador MA (1993) In: Proc. 21st Biennial Conf. on Carbon, Buffalo, NY, June 13–18
Johnson RE (1959) J Phys Chem 63:1655
Kerans RJ, Hays RS, Pagano NJ, Parthasarathy TA (1991) Am Ceram Soc Bull 68:429
Kerans RJ, Parthasarathy TA (1991) J Am Ceram Soc 74:1585
Lara-Curzio E, Ferber MK (1994) J Mater Sci 29:6158
Marshall DB, Shaw MC, Morris WL (1992) Acta Met Mater 40:443
Penn LS, Lee SM (1989) J Comp Tech & Res 11:23
Schoene C, Scala E (1970) Met Trans 1:3466
Vennett RM, Wolf SM, Levitt AP (1970) Met Trans 1:1569
Vogelsang M, Arsenault RJ, Fisher RM (1986) Met Trans A 17:379
Walter JL, Cline HE, Koch E (1969) Trans AIME 245:2073
Weihs TP, Nix WD (1991) J Am Ceram Soc 74:524
Wenzel RN (1936) Ind Eng Chem 28:987

Further Reading

Adams DF, Carlsson LA, Pipes RB (1998) Experimental characterization of advanced composite materials, 3rd edn. CRC, Boca Raton, FL
Faber KT (1997) Annu Rev Mater Sci 27:499

Kim J-K, Mai Y-W (1998) Engineered interfaces in fiber reinforced composites. Elsevier, New York
Plueddemann EP (ed) (1974) Interfaces in polymer matrix composites (vol 6 of the series Composite Materials), Academic, New York
Stokes RJ, Evans DF (1997) Fundmentals of interfacial engineering. Wiley-VCH, New York
Wagner HD, Marom G (eds) (1997) Composite interfaces (special issue—selected papers from the sixth international conference on composite interfaces (ICCI-6), Israel). VSP, Zeist, The Netherlands

Problems

4.1. Describe some techniques for measuring interfacial energies in different composite systems.
4.2. In order to study the interfacial reactions between the fiber and matrix, oftentimes one uses very high temperatures in order to reduce the time necessary for the experiment. What are the objections to such accelerated tests?
4.3. What are the objections to the use of short beam shear test to measure the interlaminar shear strength (ILSS)?
4.4. Diffusion along free surface is faster than in the bulk of a material. Similarly, diffusion along a grain boundary is faster than in the lattice. Taking these factors into account, write an expression for diffusion coefficients in order of descent for diffusion along lattice, dislocation, grain boundary, reinforcement/matrix interface, and surface. Explain the reason behind your answer.
4.5. Discuss the importance of moisture diffusion in fiber reinforced polymer matrix composites. Recall that moisture absorption in PMCs is largely due to the permeability of the polymer matrix. Suggest some possible effects of moisture absorption in fiber reinforced PMCs in terms of effects on different moduli (along the fiber and perpendicular to the fiber) and ILSS.